

Submitted to Astrophysical Journal

# Extrasolar Planets in Mean-Motion Resonance: Apses Alignment and Asymmetric Stationary Solutions

C. Beaugé<sup>1</sup>

*Observatorio Astronómico, Universidad Nacional de Córdoba, Laprida 854, (5000)  
Córdoba, Argentina*

and

S. Ferraz-Mello and T.A. Michtchenko

*Instituto Astronômico, Geofísico e Ciências Atmosféricas, Universidade de São Paulo, Rua  
do Matão 1226, 05508-900 São Paulo, Brasil*

## ABSTRACT

In recent years several pairs of extrasolar planets have been discovered in the vicinity of mean-motion commensurabilities. In some cases, such as the *Gliese 876* system, the planets seem to be trapped in a stationary solution, the system exhibiting a simultaneous libration of the resonant angle  $\theta_1 = 2\lambda_2 - \lambda_1 - \varpi_1$  and of the relative position of the pericenters.

In this paper we analyze the existence and location of these stable solutions, for the 2/1 and 3/1 resonances, as function of the masses and orbital elements of both planets. This is undertaken via an analytical model for the resonant Hamiltonian function. The results are compared with those of numerical simulations of the exact equations.

In the 2/1 commensurability, we show the existence of three principal families of stationary solutions: *(i)* aligned orbits, in which  $\theta_1$  and  $\varpi_1 - \varpi_2$  both librate around zero, *(ii)* anti-aligned orbits, in which  $\theta_1 = 0$  and the difference in pericenter is 180 degrees, and *(iii)* asymmetric stationary solutions, where both the resonant angle and  $\varpi_1 - \varpi_2$  are constants with values different of 0 or 180 degrees. Each family exists in a different domain of values of the mass ratio and eccentricities of both planets. Similar results are also found in the 3/1 resonance.

---

<sup>1</sup>Present address: Instituto Nacional de Pesquisas Espaciais (INPE), Av. dos Astronautas 1758, (12227-010) São José dos Campos, SP, Brasil

We discuss the application of these results to the extrasolar planetary systems and develop a chart of possible planetary orbits with apsidal corotation. We estimate, also, the maximum planetary masses in order that the stationary solutions are dynamically stable.

*Subject headings:* Celestial Mechanics, Extrasolar planets, Resonances.

## 1. Introduction

As the number of known extrasolar planets continues to grow, so does the discovery of multiple systems in which more than one planet seems to orbit the star. As of October 2002, ten planetary systems are known around main sequence stars, each with two or three members.

From the point of view of Celestial Mechanics, the most interesting cases are those in which two of the planets have orbital periods which are commensurable. Four extrasolar systems seem to satisfy this condition: *Gliese 876*, *HD 82943*, *55 Cnc* and *47 Uma*. The first two correspond to a 2/1 resonance, the third to a 3/1 commensurability, while the latter is close to a 5/2 relationship. With regards to *Gliese 876*, numerical simulations (Laughlin and Chambers 2001, Lee and Peale 2002a) seem to indicate that these bodies are actually trapped in a stationary solution, sometimes referred to as an *apsidal corotation*: they exhibit not only a libration of the resonant angle  $\theta_1 = 2\lambda_2 - \lambda_1 - \varpi_1$ , but also an alignment of their major axes. System *HD 82943* also shows two planets in a 2/1 commensurability relation (Butler *et al.* 2002), although in this case it is unclear whether the observed motion is also an apsidal corotation or a simple  $\theta_1$ -libration. Similar doubts also exist for the planets located in other resonances.

Although to date there is no agreement as to the origin of these resonant configurations (see Perryman 2000 for a review of the different hypotheses), it is generally believed that the planets did not form at their present observed locations, but were driven (or trapped) into the resonances during a migration process triggered by some non-conservative force. Whether this orbital drift is still at work is also a matter of debate, although it is more plausible to assume that it stopped after the end of the planetary formation stage. However, and independently of how they reached this point, an important consequence of this type of configuration is that it constitutes a stabilizing mechanism for planetary orbits, especially if they have large eccentricities.

In the last few years, several studies have been performed to find initial conditions that yield stable stationary solutions. Since the observational data usually does not yield explicit

values for the masses, these tests are very important to estimate upper bounds for these parameters, as well as indications for limits in the inclination of the orbital plane of the planetary system. One of the first analysis is due to Hadjidemetriou (2001), who studied the stability of numerically generated families of periodic orbits in the planar-elliptic 2/1 resonance. The results were later applied to both the *Gliese 876* and the *HD 82943* systems. Lee and Peale (2002a) presented a model for the *Gliese 876* system, and studied the capture of these planets into the resonance by an inward orbital migration. This trapping may explain the present apsidal corotation configuration, as well as the large eccentricity shown by both planets. The model was based on a Laplacian expansion of the disturbing function, truncated at third order in the eccentricities. The resulting equations were then used to discuss the existence and location of stationary solutions in the averaged (resonant) phase space. The authors concluded that two types of stable configurations exist: (i) for quasi-circular orbits such as the Io-Europa system, the corotation point lies in the axis  $\varpi_1 - \varpi_2 = 180$  degrees; (ii) for sufficiently large values of the eccentricities the stable solution occurs for  $\varpi_1 - \varpi_2 = 0$ . In both cases, the resonant angle  $\theta_1$  librates around zero. Similar results have also been presented by Murray *et al.* (2001).

It is important to bear in mind, however, that the Laplace expansion of the disturbing function is not convergent for large values of the eccentricities. In the case of the 2/1 resonance, the applicability of this model is restricted to eccentricities below 0.17 (see Ferraz-Mello 1994). For larger values, a truncated expansion may yield even qualitatively incorrect results (Beaugé 1994). Although this limit may not seem important in the case of our own Solar System where planets move in quasi-circular orbits, the same does not hold for extrasolar systems where highly elliptic motions abound. Even planets trapped in resonances show highly eccentric orbits. In *Gliese 876*, the best dynamical fits of observational data place the eccentricity of the inner planet at values of the order of 0.25 – 0.32. For *HD 82943* it seems even worse, since these values may reach 0.41 – 0.54.

The aim of the present work is to develop an adequate analytical model for the study of planetary mean-motion resonances, even in the high-eccentricity case. We will then search for all possible stable stationary solutions in terms of the orbital elements and masses, without mentioning possible resonance trapping mechanisms. Thus, we shall not indulge in how the planets may have reached these solutions, our interest lying only in what these solutions look like and where they are located. The ultimate goal will be to present a “chart” or a “map” of all the possible locations of planets in apsidal corotation, as a function of their eccentricities and mass ratios. With such a tool, we will be able to obtain a better idea of the permissible orbits of extrasolar planets. Under certain hypotheses, it will be possible to ascertain whether orbits deduced via data analysis of the observations are in fact plausible without having to resort to long-term numerical simulations for different masses.

This manuscript is divided as follows: In Section 2 we introduce the problem and the physical system under study. The analytical model is introduced in Section 3, where the conditions for corotational solutions are described. Application of the model to the 2/1 resonance, and results, are shown in Section 4. The case of the 3/1 resonance is discussed in Section 5. Finally, conclusions close the paper in Section 6.

## 2. The General Three-Body Problem

Suppose two planets of masses  $m_1$  and  $m_2$  orbiting a star of mass  $M_0 \gg m_1, m_2$ . Of course, the same dynamical system could be said to represent two massive satellites orbiting a planet. Both problems are equivalent from the dynamical point of view. However, since we are primarily interested in analyzing the case of extrasolar planets, throughout this paper we refer to  $M_0$  as the star and  $m_1, m_2$  as the planets.

This system is a particular case of the general three-body problem and is different of the restricted problems in which one of the bodies is supposed to have a negligible mass. We will consider two approximations. First, we will disregard oblateness effects of the central star and the planets, and thus consider only the mutual gravitational perturbations in the point-mass approximation. This limitation may be important if the secondary bodies orbit very close to the central body. Second, we will suppose all motion planar. This restriction does not seem to be significant, since the massive resonant planetary satellites have practically no inclination with respect to the equator. For extrasolar planets, their mutual inclination is not known with any precision, and is usually taken equal to zero.

Let  $a_i$  denote the semimajor axis of the  $i^{\text{th}}$ -planet ( $i = 1, 2$ ),  $e_i$  the eccentricity,  $\lambda_i$  the mean longitude and  $\varpi_i$  the longitude of the pericenter. All orbital elements will be referred to the central star  $M_0$ . We will suppose  $a_1 < a_2$ , thus the subscript 2 will correspond to the outer orbiting body. This is a four degree of freedom system and its dynamical evolution can be specified by eight variables. In terms of the orbital elements of both planets, these can be given by the set  $(a_1, a_2, e_1, e_2, \lambda_1, \lambda_2, \varpi_1, \varpi_2)$ . Two integrals of motion exist: the total energy (or analogously, the Hamiltonian function  $F$ ), and the total angular momentum  $J_{\text{tot}}$ .

Imagine now that both planets lie in the vicinity of a generic mean-motion commensurability  $(p+q)/p$  with  $q \neq 0$ . In other words, let their mean motions  $n_i$  satisfy the relationship  $(p+q)n_2 - pn_1 \sim 0$ . In terms of their orbital elements, we can then define what is usually referred to as the *resonant* or *critical* angles of the system:

$$\begin{aligned} q\sigma_1 &= (p+q)\lambda_2 - p\lambda_1 - q\varpi_1 \\ q\sigma_2 &= (p+q)\lambda_2 - p\lambda_1 - q\varpi_2 \end{aligned} \tag{1}$$

Since  $\sigma_2 - \sigma_1 = \varpi_1 - \varpi_2 = \Delta\varpi$ , sometimes it is better to substitute the variable  $\sigma_2$  with the difference in longitude of pericenter  $\Delta\varpi$ . Similarly, since the resonant angle  $\sigma_1$  always appears in the disturbing function multiplied by the order of the resonance  $q$ , it is also common practice to introduce new variables  $\theta_i = q\sigma_i$ . With these changes in mind, we will consider  $\theta_1$  and  $\Delta\varpi$  as the slow angles of the problem. The fast angles, associated with the synodic period of the system, are usually eliminated by means of an averaging process.

### 3. The Analytical Model

In a recent study, Beaugé and Michtchenko (2002) presented an analytical model for the Hamiltonian  $F$  of the planetary three-body problem. At variance with classical expansions, this function is valid even for high values of the eccentricities of both planetary bodies, up to a limit of about  $e_i \sim 0.5$ . This limit varies according to the ratio  $a_1/a_2$ , being smaller for planets closer one to the other. We will then begin this section reviewing the form of this function.

#### 3.1. The Resonant Hamiltonian

In Section 2, we mentioned that the averaged system in resonance can be specified by two angular variables, for example,  $(\sigma_1, \sigma_2)$ . Their canonical conjugates are given by:

$$I_i = L_i \left( 1 - \sqrt{1 - e_i^2} \right) \quad (i = 1, 2). \quad (2)$$

Here  $L_i = m'_i \sqrt{\mu_i a_i}$  is the modified Delaunay action related to the semimajor axis in Poincaré variables (see Laskar 1991),  $\mu_i = G(M_0 + m_i)$ , and  $G$  is the gravitational constant. The factor  $m'_i$  is a reduced mass of each body, given by:

$$m'_i = \frac{m_i M_0}{m_i + M_0}. \quad (3)$$

For small values of the eccentricities,  $I_i \sim L_i e_i^2 / 2$ . Thus, for fixed values of the semimajor axes, the momenta  $I_i$  are proportional to the square of the eccentricities.

In this resonant case, the Hamiltonian  $F$  defines a two degree-of-freedom system in the canonical variables  $(I_1, I_2, \sigma_1, \sigma_2)$ . Apart from the Hamiltonian itself, two other integrals of motion exist in this averaged problem:

$$\begin{aligned} J_1 &= L_1 + (p/q)(I_1 + I_2) = \text{const} \\ J_2 &= L_2 - (1 + p/q)(I_1 + I_2) = \text{const} \end{aligned} \quad (4)$$

such that  $J_{\text{tot}} = J_1 + J_2$  (Michtchenko and Ferraz-Mello 2001). With these definitions, the complete Hamiltonian of the system, averaged over short-period terms, can be expressed as:

$$F = - \sum_{i=1}^2 \frac{\mu_i^2 m_i'^3}{2L_i^2} - F_1, \quad (5)$$

where the disturbing function  $F_1$  can be expressed by means of the truncated series

$$F_1 = \frac{Gm_1m_2}{a_2} \sum_{j,k,l,u,s} R_{j,k,l,u,s} (\alpha - \alpha_0)^j \cdot e_1^k e_2^l \cos(uq\sigma_1 + s(\sigma_2 - \sigma_1)). \quad (6)$$

For a given resonance, the coefficients  $R_{j,k,l,u,s}$  are constant for all initial conditions. The variable  $\alpha = a_1/a_2$  denotes the ratio between semimajor axes, and  $\alpha_0$  is its value at exact resonance. In the summations, the first four index vary from zero to a maximum value which is user-specified. The last index (i.e.  $s$ ) takes both positive and negative values, whose limit can also be modified according to the desired precision. For details on the construction of this expression, the reader is referred to Beaugé and Michtchenko (2002).

### 3.2. Stationary Solutions

Figure 1 shows level curves of constant Hamiltonian  $F$  for the 2/1 resonance, as function of both angular variables, and for fixed values of the planetary eccentricities. The top plot corresponds to  $e_1 = e_2 = 0.02$  while the bottom graph presents results for  $e_1 = e_2 = 0.1$ . These contour plots give a general idea of the topology of the system, and help identify possible stationary solutions (seen here as full circles). This topology changes significantly from one plot to the other. The geometry of Figure 1(a) is what is expected in the so-called low-eccentricity regime, as is the case of the Io-Europa pair, and in which the stable stationary solution occurs at  $\theta_1 = \sigma_1 = 0$  and  $\Delta\varpi = 180$  degrees. The bottom plot presents a different story. At the place of the previous stable solution, now appears an unstable solution (i.e. a saddle point). The solution bifurcated into two new ones. These new stable solutions are located outside the central axes of the figure and correspond, in the case shown, to the values  $\theta_1 \simeq \pm 15$  degrees and  $\Delta\varpi \simeq 180 \pm 80$  degrees. These are what we can call *asymmetric* stationary solutions.

In order to study in detail the existence and location of all these stationary solutions, we must make use of the equations of motion of the Hamiltonian system. These are given by:

$$\frac{dI_i}{dt} = -\frac{\partial F}{\partial \sigma_i} \quad ; \quad \frac{d\sigma_i}{dt} = \frac{\partial F}{\partial I_i} \quad (i = 1, 2). \quad (7)$$

Thus, the stationary solutions will be given by the conditions:

$$\frac{\partial F}{\partial \sigma_i} = \frac{\partial F}{\partial I_i} = 0 \quad (i = 1, 2) \quad (8)$$

and their stability defined by the behavior of the Hessian of  $F$  evaluated at the point. These stationary solutions, or *apsidal corotation solutions*, are fixed points in the averaged system. When we reintroduce the short-period terms, they become periodic orbits in real space, whose period is simply the synodic period of the problem.

Before discussing these equations, let us simplify them introducing a change in units. First, we will consider  $M_0$  as the unit of mass, and the planetary masses  $m_i$  will now be expressed in terms of the central mass. Second, we will set  $a_2$  as the unit distance. Thus,  $a_1 = \alpha$ . These modifications will imply a new numerical value for  $G$  but, otherwise, the equations and coefficients are preserved. To search for the stationary solutions, let us discuss separately the derivatives with respect to the angles, and those with respect to the momenta. In the first one, since the two-body Hamiltonian contribution is independent of  $\sigma_i$ , we simply have that:

$$\begin{aligned} 0 = \frac{\partial F_1}{\partial \sigma_1} &= Gm_1m_2 \sum_{j,k,l,u,s} (uq - s)R_{j,k,l,u,s}(\alpha - \alpha_0)^j \\ &\quad \cdot e_1^k e_2^l \sin(u\theta_1 + s\Delta\varpi) \\ 0 = \frac{\partial F_1}{\partial \sigma_2} &= Gm_1m_2 \sum_{j,k,l,u,s} sR_{j,k,l,u,s}(\alpha - \alpha_0)^j \\ &\quad \cdot e_1^k e_2^l \sin(u\theta_1 + s\Delta\varpi) \end{aligned} \quad (9)$$

where we have substituted  $\theta_1 = q\sigma_1$  and  $(\sigma_2 - \sigma_1) = \Delta\varpi$ . The right-hand sides of both equations are directly proportional to the product of the masses and the gravitational constant. Since the terms inside the sums are independent of these parameters, the algebraic equations (9) constrain the values of  $\alpha - \alpha_0, e_1, e_2, \theta_1, \Delta\varpi$ . If we forget, for the time being, the dependence with the semimajor axis (fixed at the exact resonance values, for instance), each given value of the pair  $(e_1, e_2)$ , lead to the values of  $\theta_1$  and  $\Delta\varpi$  such that equation (9) is satisfied.

Independently of  $(e_1, e_2)$ , equations (9) contain a set of trivial solutions, given by  $\theta_1 = 0$  or  $180$  and  $\Delta\varpi = 0$  or  $180$  (units are in degrees), although not all of them are stable. Depending on the eccentricities, in certain cases  $\theta_1 = 0, \Delta\varpi = 0$  will be stable. In others, the stability will appear in  $\theta_1 = 0, \Delta\varpi = 180$ . In yet other cases, as seen in Figure 1(bottom), all those solutions will be unstable.

If our expansion of the Hamiltonian function were restricted to a single harmonic in each angular variable (i.e.  $u_{max} = s_{max} = 1$ ), as is usually the case in most simplified models,

then symmetric solutions would be the only possible solution for system (9). Nevertheless, if we consider a larger number of periodic terms, then it is possible, for certain values of  $(e_1, e_2)$ , to find zeros of these derivatives for values of  $\theta_1$  and  $\Delta\varpi$  different from 0 or 180 degrees.

Let us now concentrate on the remaining two equations of system (8). They are:

$$\begin{aligned} 0 = \frac{\partial F}{\partial I_1} &= \sum_{i=1}^2 \frac{\mu_i^2 m_i'^3}{L_i^3} \frac{\partial L_i}{\partial I_1} + \frac{\partial F_1}{\partial I_1} \\ &= \frac{p}{q} \mu_1 n_1 - \left(1 + \frac{p}{q}\right) \mu_2 n_2 + \frac{\partial F_1}{\partial I_1} \\ 0 = \frac{\partial F}{\partial I_2} &= \sum_{i=1}^2 \frac{\mu_i^2 m_i'^3}{L_i^3} \frac{\partial L_i}{\partial I_2} + \frac{\partial F_1}{\partial I_2} \\ &= \frac{p}{q} \mu_1 n_1 - \left(1 + \frac{p}{q}\right) \mu_2 n_2 + \frac{\partial F_1}{\partial I_2} \end{aligned} \tag{10}$$

where  $n_i$  are the mean motions of the planets. Once again, the right-hand sides depend on both the orbital elements and the masses. We can write this explicitly saying that algebraic equations (10) constrain the set

$$(e_1, e_2, \theta_1, \Delta\varpi, \alpha, m_1/m_2, m_1). \tag{11}$$

In our own Solar System, the values of  $m_1/m_2$  and  $m_1$  are known with a high precision; they are not considered variables but known *parameters* of the problem. In such a case, it is common practice to choose a value of  $\alpha$  and use equations (9)-(10) to obtain the equilibrium values of  $(e_1, e_2, \theta_1, \Delta\varpi)$  for each semimajor axis. The problem of extrasolar planets is different. Here, the individual masses of the bodies are usually not known, and only their ratio is estimated by the observational data. For this reason, a change of strategy is necessary.

In the following sections we will determine the solutions as parametrized by (supposedly unknown) values of  $m_1$ . In other words, we will consider a certain value for the mass of the inner body, solve the algebraic equations, and then study the variation of these solutions for different values of this parameter. In each case, we will analyze the plane defined by the eccentricities of both planets  $(e_1, e_2)$ , and for each point of this pair we will solve the algebraic conditions for apsidal corotations to obtain the (stable) stationary values of  $(\theta_1, \Delta\varpi, \alpha, m_1/m_2)$ . Consequently, for all the points in the plane of the orbital eccentricities, we will be able to plot level curves of the values of the angles and the ratio of the masses.



## 4. Results for the 2/1 Resonance

We begin analyzing the resonant solutions in which both longitudes of pericenter appear aligned or anti-aligned. Initially, we took the inner mass equal to  $m_1 = 10^{-4}M_0$ . Then, for each value of the pair  $(e_1, e_2)$ , we used equations (9)-(10) to determine which symmetric apsidal solution corresponds to an extreme value of the Hamiltonian function. This procedure was repeated for a grid of eccentricities in the range  $e_i \in [0, 0.4]$ .

### 4.1. Apsidal Corotations with Anti-Aligned Pericenters

Results for anti-aligned apsidal corotations are shown in Figure 2. It can be seen that all solutions lie beneath a fairly straight broad curve, and are located at small values of the eccentricities. Inside this region, we have plotted the level curves of constant values of  $m_2/m_1$ . Thus, for example, for  $e_1 = 0.06$ , all solutions with  $e_2 < 0.014$  correspond to stable apsidal corotations for some value of  $m_2/m_1$ . Conversely, if  $e_2 > 0.014$ , no stationary solution of this type exists, whatever the mass ratio of the planets.

The level curves themselves also yield important information. For example, they show that in most of this region, the stable solutions correspond to cases where the mass of the exterior planet is smaller than that of the inner one. In the limit where  $m_2/m_1 \rightarrow 0$ , all solutions tend to  $e_1 = 0$ . In the opposite case, when  $m_2 \gg m_1$ , these corotations occur for small values of  $e_2$ . Thus, in the limit where the general three-body problem tends towards the restricted case, the eccentricity of the massive perturber must be very small to allow the pericenters to be anti-aligned.

### 4.2. Apsidal Corotations with Aligned Pericenters

In Figure 3 we present analogous results, now in the case where  $\Delta\varpi = 0$ . Once again, all the solutions occur for values of  $(e_1, e_2)$  beneath a broad black curve, but  $e_1$  is no longer limited to small values. In fact, this type of solution only occurs for eccentricities of the inner planet larger than  $\sim 0.097$ . The level curves of constant mass-ratio show that practically all the points correspond to  $m_2 > m_1$ . Solutions with  $m_2 < m_1$  are also present, although these tend asymptotically to the thick curve as the ratio  $m_2/m_1$  approaches unity.

As a comparison of the model's results with numerical data, we also present in this graph (full circles) the best dynamical fits of the two planets of the *Gliese 876* system (Laughlin and Chambers 2001). What we call *Fit 1* refers to the dynamical fit with Keck+Lick observations

and an inclination of the system’s orbital plane equal to  $\sin i = 0.78$ . *Fit2* corresponds to the Keck data only, and a value of  $\sin i = 0.55$ . Both solutions fall well within the region of aligned pericenters, as predicted by Lee and Peale (2002a). However, they do not correspond to the mass ratio corresponding to an exact apsidal corotation. From the observational data,  $m_2/m_1 \simeq 3.15$ . Comparing it to our results, this shows a very good agreement with the level curves of *Fit 1*, although not so good for the second one. This discrepancy is probably due to the fact that the orbits deduced from the Keck data do not correspond to an exact corotation, but display a significant amplitude of libration of both angles. In other words, the solution does not lie at the maximum of  $F$  (see Figure 1(top)) but corresponds to one of the closed curves around that point.

With regards to this point, it is important to recall the alleged origin of this resonant configuration. If, as generally believed, these planets were trapped in the apsidal corotation through the action of non-conservative forces, then it is expected that the bodies would have evolved towards an extreme value of the total energy (i.e. Hamiltonian). In other words, the observed corotation should correspond to a zero-amplitude solution. A look at the numerical simulations of Lee and Peale (2002a) shows that the adopted values of eccentricities and mass ratio of the planets does not yield such a zero-amplitude solution. This does not mean that the orbits are unstable; just that they are not extremes of the total energy. Consequently, either the dynamical fits are correct and the planets are not exactly at corotation, or the orbital elements of the planets must be modified to bring them to a stationary solution associated to the observed mass ratio.

Finally, from the practitioner’s point of view, the most important aspect of Figures 2 and 3 is that they constitute a “chart” of possible solutions, as function of observable quantities such as the eccentricities and the ratio of masses. For example, if the observational data of a given planetary system in the 2/1 resonance yields a certain value of  $e_1, e_2$  and  $m_2/m_1$ , we can check them against these plots and confirm whether they do indeed correspond to a stable apsidal corotation solution. This information can be obtained without having to resort to numerical simulations of the dynamical evolution of the system.

### 4.3. Asymmetric Stationary Solutions

We have seen that the limit of the regions of solutions with anti-aligned and aligned pericenters are given by two curves stemming from the point  $(e_1, e_2) \sim (0.097, 0.000)$ . The first are located in the interval  $e_1 < 0.097$  and for  $e_2$  beneath the corresponding curve. Aligned solutions are restricted to the open interval  $e_1 > 0.097$ . Above these broad curves all symmetric apsidal corotations are unstable, and we enter the realm of the asymmetric

corotations. These new apsidal corotation solutions are shown in Figure 4, where once again we present solutions in the plane  $(e_1, e_2)$ . The top graph shows the values of  $e_1, e_2$  corresponding to a same resonant angle  $\theta_1$ , while the bottom plot presents those with a same  $\Delta\varpi$ . All angles are given in degrees.

These results were obtained solving the algebraic system (9). We may use equations (10) to assign a mass ratio  $m_2/m_1$  to each pair of eccentricities. The results are shown in Figure 5 once again in the form of a contour plot. We can see that practically all solutions occur for exterior planets smaller than interior ones. A small region of  $m_2/m_1 > 1$  is present very close to the limit with the aligned apsidal corotations, although they exist only for values very close to unity. However, they are important in the sense that asymmetrical corotations can in fact exist in such a case. Also seen in this graph, the diagonal broken line shows the values of the eccentricities for which both orbits intersect, but are protected from a collision by the resonance.

Simultaneously with the mass ratio, equations (10) also gives the stationary values of  $\alpha$ . With them, we may, now, return to the algebraic system (9) and determine corrected values of the angular variables. These second-order corrections, however, never exceed 0.1 degrees. Thus, unless extremely precise values are needed, it is safe to consider all the results in Figure 4 as virtually independent of the planetary masses.

As a final note, let us point out that, due to the symmetries of the problem, if  $\theta_1$  is a solution of the system, so is  $360 - \theta_1$ . The same applies to the difference in pericenter. Although all these solutions may be grouped by plotting  $|\theta_1| = \text{const}$  and  $|\Delta\varpi| = \text{const}$ , it is important to stress that each solution constitutes an individually distinct corotation created by the bifurcation in the location of the maximum of  $F$  as shown in Figure 1.

#### 4.4. Global View of the Apsidal Corotations

These contour-plots give a global view of all possible solutions showing apsidal corotations for eccentricities up to 0.4. We can divide the plane in three regions. Symmetric solutions are categorized in regions **A** and **B**, according whether they correspond to an alignment or anti-alignment of the pericenters. The region above them corresponds to asymmetric corotations. With respect to the resonant angle, all symmetric solutions have  $\theta_1 = 0$ . The non-symmetric solutions have  $\theta_1 \sim 0$  for the values of  $e_2$  immediately above the value corresponds to the broad curves. The stationary value of  $\theta_1$  grows primarily with the eccentricity of the outer planet, reaching a maximum of about 60 degrees for  $(e_1, e_2) \simeq (0, 0.4)$ . The blank region at the upper right-hand side of the graph corresponds to high values of both

eccentricities and is close to the limit of the model. The level curves of  $\Delta\varpi$  show a different behavior. Since this angle is equal to 180 degrees in the region **A**, and equal to zero in **B**, the asymmetric solutions also follow this trend and cover all the numerical values between these two extremes. At variance with the previous plot, the contours now seem to be more dependent on  $e_1$  than on  $e_2$ .

We have also performed several numerical simulations of the capture process in the 2/1 resonance, using different mass ratios and initial conditions (Ferraz-Mello *et al.* 2002). Figure 6 shows a typical result obtained with  $m_2/m_1 \simeq 0.54$ , which is equal to the mass ratio of the Jovian satellites Io and Europa. On the top graph, we show the temporal evolution of  $\alpha = a_1/a_2$ . Both planets began the simulation in circular orbits with a mutual separation larger than that corresponding to the 2/1 commensurability. The semimajor axis of the inner body was then slowly increased due to the action of an anti-dissipative force pumping orbital energy into the system. When the value of  $\alpha$  reached the resonance (at approximately  $t = 100$ ) the capture occurred and, from this point onwards, the ratio of semimajor axes remained fixed. Figure 6b shows the behavior of both eccentricities. When the trapping occurs,  $e_1$  begins to grow while the eccentricity of the outer planet remains close to zero. A look at plots (c) and (d) show that this interval corresponds to symmetric apsidal corotations. The solution is first trapped in  $\theta_1 = 0$  and  $\Delta\varpi = 180$  degrees. However, at  $t \sim 300$  years, the relative perihelia positions reverse and they become aligned ( $\Delta\varpi = 0$ ). This corresponds to an evolution from region **A** to region **B** (see Figure 4).

When the value of  $e_1$  reaches  $\sim 0.15$ , the system leaves the domain of symmetric apsidal corotations and enters that of asymmetric ones. Both eccentricities now begin to grow significantly and the angular variables  $\theta_1$  and  $\Delta\varpi$  vary, taking values along the corresponding family of asymmetric apsidal corotations. This behavior continues up to near the end of the simulation, when the system returns to have anti-aligned apses. Similar numerical results have been presented recently by Lee and Peale (2002b).

Finally, Figure 6(e) shows  $e_2$  as function of  $e_1$  for all the stationary solutions attained by the system during its evolution, allowing a direct comparison with the analytical model (see Figure 5). As a reference, we have also plotted (broken lines) the limits between the domains of symmetric and asymmetric solutions, as deduced from our equations.

#### 4.5. Dependence with the Actual Planetary Masses

So far, we have determined all the solutions considering a fixed value of  $m_1 = 10^{-4}$ . We will now vary this mass and see its effect on our results. Recall that the stationary values

of  $\theta_1, \Delta\varpi$  are practically invariant to this change. However, for a given pair  $e_1, e_2$ , the mass ratio  $m_2/m_1$  may depend on this parameter. To see this dependence, we analyzed a few corotational solutions (chosen such that  $e_1 = e_2$ ). For each, we took values of the inner mass in the range  $\log(m_1/M_0) \in [-5, 0]$ , and determined the mass ratio corresponding to a stationary solution. The results are shown in Figure 7. We can see that the dependence of the solution with  $m_1$  is very weak, never exceeding 1%. In other words, the corotational solutions determined for one value of  $m_1$  will suffer practically no change if this value is changed.

This has two main consequences. First, the results presented in Figures 2-4 are practically independent of the individual masses of the system. Thus, they are very general and should be applicable to practically any planetary system found in a 2/1 resonance. However, this lack of sensitivity of the results implies also that it is not possible to deduce the individual masses from the fact that a given system lies in an exact apsidal corotation.

Second, note that for each value of  $e$  there exists a maximum value of  $m_1$  for which the stable corotations exist. The variation of this critical value of  $m_1$  in the plane  $(e_1, e_2)$  is shown in Figure 8 as level curves. In the interval of eccentricities considered, all limit values are very similar, and of the order of  $\sim 0.01 - 0.02M_0$ . If the individual mass of the inner planet is larger than this limit, then the apsidal corotation solutions become unstable. This places some dynamical limit on the values of the individual planets showing apsidal corotations, and not just on their mass ratio. Although not very restrictive, this limit is enough to exclude for brown dwarfs.

## 5. The 3/1 Resonance

Extrasolar planets are not only found in the vicinity of the 2/1 commensurability, but also around other resonances. In particular, the *55 Cnc* system seems to contain three planets, two of which orbiting very close to a 3/1 resonance. Different four-body dynamical fits yield eccentricities of the order of  $0.013 - 0.039$  for the inner mass, and  $0.080 - 0.157$  for the outer. Masses are of the order of  $0.83M_{Jup}$  and  $0.20M_{Jup}$ , respectively.

In this section we will determine the apsidal corotations of the 3/1 commensurability, in the same manner as discussed for the 2/1 resonance. The equations of motion and conditions for equilibrium are analogous; the only care we must take is to change the values of  $p$  and  $q$ . For this configuration,  $p = 1$  and  $q = 2$ . It is important to recall that, in the asteroidal case, all exterior resonances of the type  $(p + q)/p = j$  (with  $j$  positive integer) have asymmetric librations (Morbidelli *et al.* 1995).

Figure 9 shows all the stable stationary values of the angular variables  $\theta_1$  and  $\Delta\varpi$  in the plane  $e_1, e_2$ . Two independent regions are evident. For all values of  $e_2 < \sim 0.13$ , apsidal corotation solutions are symmetric and occur for  $\theta_1 = 180$  and  $\Delta\varpi = 180$  degrees. However, if the eccentricity of the inner planet is larger than the limit  $e_2 \simeq 0.13$ , the stationary solutions become asymmetric. It is interesting to note that, at variance with the 2/1 case, the limit between both domains is practically independent of  $e_1$ .

The mass ratio of both planets corresponding to these solutions is shown in Figure 10. The contour plots are close to piecewise straight lines, with a slope discontinuity at the boundary of the two regions. One may note that  $e_2 \rightarrow 0$ , the value of  $m_2/m_1$ -ratio of the apsidal corotation solutions approaches and the used model becomes the so-called interior asteroid problem. Conversely, when  $e_1 \rightarrow 0$  the mass ratio is smaller than unity. Although symmetric solutions show a preponderance of systems with  $m_2 > m_1$ , and the inverse occurs in asymmetric orbits, in both cases we can see examples with all values of the mass ratio.

## 6. Conclusions

We have presented, in this paper, analytical and numerical results on the existence and location of stable stationary solutions, in the averaged planetary three-body problem, around the 2/1 and 3/1 mean-motion resonances. We have shown the existence of two distinct type of solutions. The first of these are symmetric apsidal corotations with , with  $\varpi_1 - \varpi_2 = 0$  (aligned periapses) or  $\varpi_1 - \varpi_2 = 180$  degrees (anti-aligned periapses); In the 2/1 resonance,  $\theta_1 = 0$ , while in the 3/1 resonance  $\theta_1 = 180$  degrees. These solutions are well known from classical studies dating from the works of Laplace in the nineteenth century. A second type of equilibrium solutions has also been found, this time characterized by asymmetric configurations, in which both the resonant angle  $\theta_1$  and  $\varpi_1 - \varpi_2$  librate around values which are not 0 or 180 degrees. Although asymmetric resonant solutions are known to occur in exterior resonances of the restricted three-body problem (see Beaugé 1994), only recently has there been any indication that they may also be present in the planetary case (Ferraz-Mello, 2002; Lee and Peale 2002b).

The plots we have presented for both commensurabilities are useful tools for the research in extrasolar planets. On one hand, they allow for a simple method for testing whether a certain dynamical fit of observational data is consistent with stable corotations. This information is obtained without having to resort to any numerical simulation of the equations of motion. As an additional example of this application, in Figure 10 we have plotted (in full circles) the three best dynamical fits of the two resonant planets of the *55Cnc* system (Marcy *et al.* 2002). Only one of them corresponds to a symmetric apsidal corotation, while the

other two lie in the asymmetric domain. Furthermore, all of them correspond to mass ratios of the order of 0.05, although from observational data it is estimated that  $m_2/m_1 \sim 0.24$ .

It is conceivable that, although these planets may be trapped in the 3/1 resonance, they do not lie in an apsidal corotation solution but in a  $\theta_1$ -libration only. In other words, they could exhibit a libration of the resonant angle  $\theta_1$  but a circulation of  $\theta_2$  and, thus, a circulation of the relative perihelion positions. The problem with this hypothesis is that all numerical simulations of the capture process of extrasolar planets have resulted in apsidal corotations and there has been no reported case of capture in  $\theta_1$ -libration only. This does not mean such solutions do not exist; perhaps their capture probability is small, or they are very sensitive to the modelization of the non-conservative force that drives the orbital migration. Hopefully, further simulations will shed new light on this question.

Finally, we have seen that although the solutions are only weakly dependent on the individual masses of the planets, there does exist a maximum value of  $m_i$  for which these are stable. This limit allows us to estimate upper bounds for the values of the masses, and thus give qualitative information about the maximum inclination of the orbital plane of the planetary systems.

This work has been supported by the Brazilian National Research Council -CNPq- through the fellowships 300953/01-1 and 300946/96-1, as well as the São Paulo State Science Foundation FAPESP. The authors gratefully acknowledge the support of the Computation Center of the University of São Paulo (LCCA-USP) for the use of their facilities.

## REFERENCES

- Beaugé, C. (1994). Asymmetric librations in exterior resonances. *Cel. Mech. & Dynam. Astron.*, **60**, 225-248.
- Beaugé, C. and Michtchenko, T.A. (2002). Modeling the high-eccentricity planetary three-body problem. *MNRAS*, submitted.
- Butler, P., Marcy, G., Vogt, S., Tinney, C., Jones, H., McCarthy, C., Penny, A., Apps, K. and Carter, B. (2002). On the double planet system around HD 83443. *ApJ*, **578**, 565-572.
- Ferraz-Mello, S. (1994). The convergence domain of the Laplacian expansion of the disturbing function. *Cel. Mech. & Dynam. Astron.*, **58**, 37-52.

- Ferraz-Mello, S. (2002). Tidal Acceleration, Rotation and Apses Alignment in Resonant Extra-Solar Planetary Systems *Bull. A.A.S.* , in press.
- Ferraz-Mello, S., Michtchenko, T.A. and Beaugé, C. (2003). Dynamics of the convergent migration of two planets under the action of anti-dissipative forces. *Cel. Mech. & Dynam. Astron.*, **87** to be published.
- Hadjidemetriou, J. (2001). Resonant periodic motion and the stability of extrasolar planetary systems. *Cel. Mech. & Dynam. Astron.*, **83**, 141-154.
- Laskar, J. (1991). Analytical framework in Poincaré variables for the motion of the Solar System. In: *Predictability, Stability and Chaos in N-Body Dynamical Systems* (A. Roy, Ed.). NATO Asi Series, Vol. B272, pp. 93-112, Plenum Press, New York.
- Laughlin, G. and Chambers, J. (2001). Short-term dynamical interactions among extrasolar planets. *ApJ*, **551**, L109-L113.
- Lee, M.H. and Peale, S.J. (2002a). Dynamics and origin of the 2:1 orbital resonances of the GJ 876 planets. *ApJ*, **567**, 596-609.
- Lee, M.H. and Peale, S.J. (2002b). Extrasolar planets and mean-motion resonances. In Scientific Frontiers in Research on Extrasolar Planets. Eds. D. Deming and S. Seager, (ASP Conf. Series), in press.
- Marcy, G.W., Butler, R.P., Fischer, D., Laughlin, G., Vogt, S.S., Henry, G.W. and Pourbaix, D. (2002). A planet at 5 AU around 55 Cancri. *ApJ*, in press.
- Michtchenko, T.A. and Ferraz-Mello, S. (2001). Modeling the 5:2 mean-motion resonance in the Jupiter-Saturn planetary system. *Icarus*, **149**, 357-374.
- Morbidelli, A., Thomas, F. and Moons, M. (1995). The resonant structure of the Kuiper belt and the dynamics of the first five trans-neptunian objects. *Icarus*, **118**, 322-340.
- Murray, N., Paskowitz, M. and Holman, M. (2001). Eccentricity evolution of resonant migrating planets. *ApJ*, **565**, 608-620.
- Perryman, M.(2000). Extra-solar planets. *Rep. on Progress in Phys.*, **63**, 1209.



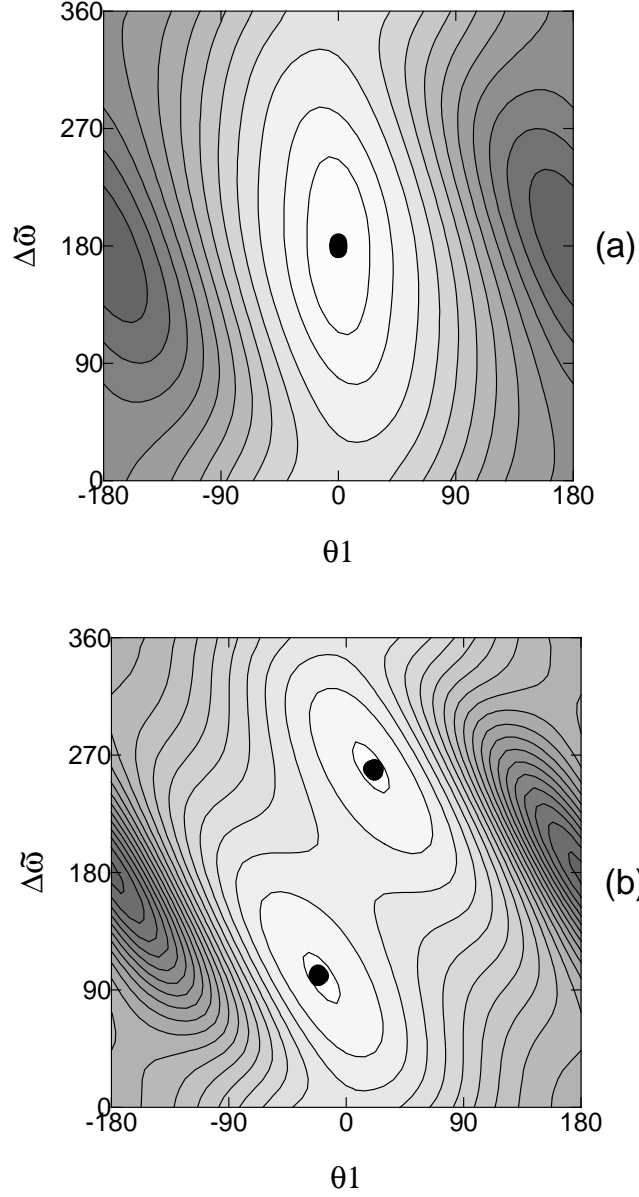


Fig. 1.— Level curves of the complete Hamiltonian function  $F$ , in the plane of  $\Delta\varpi$  vs.  $\theta_1$ . Top graph corresponds to eccentricities equal to  $e_1 = e_2 = 0.02$ , while bottom plot shows the results for  $e_1 = e_2 = 0.1$ . Lighter shades of gray indicate larger values of the function. Stable stationary solutions (maxima of  $F$ ) are shown by dots.

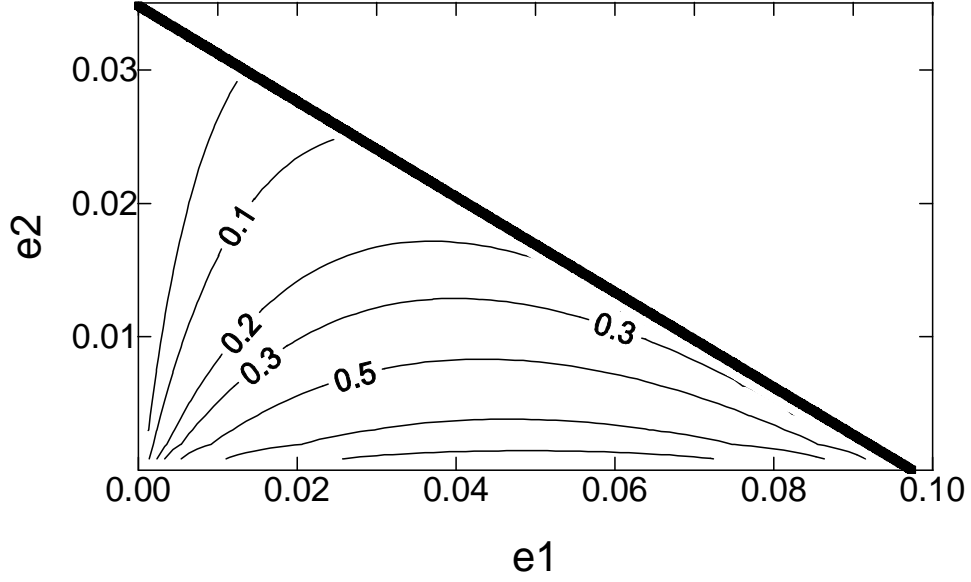


Fig. 2.— Anti-aligned corotation solutions ( $\Delta\varpi = 180$ ), for the 2/1 resonance, in the plane  $(e_1, e_2)$ . The level curves correspond to constant values of the mass ratio  $m_2/m_1$ . The region is delimited by the thick black curve, above which no stable symmetric solution exist.

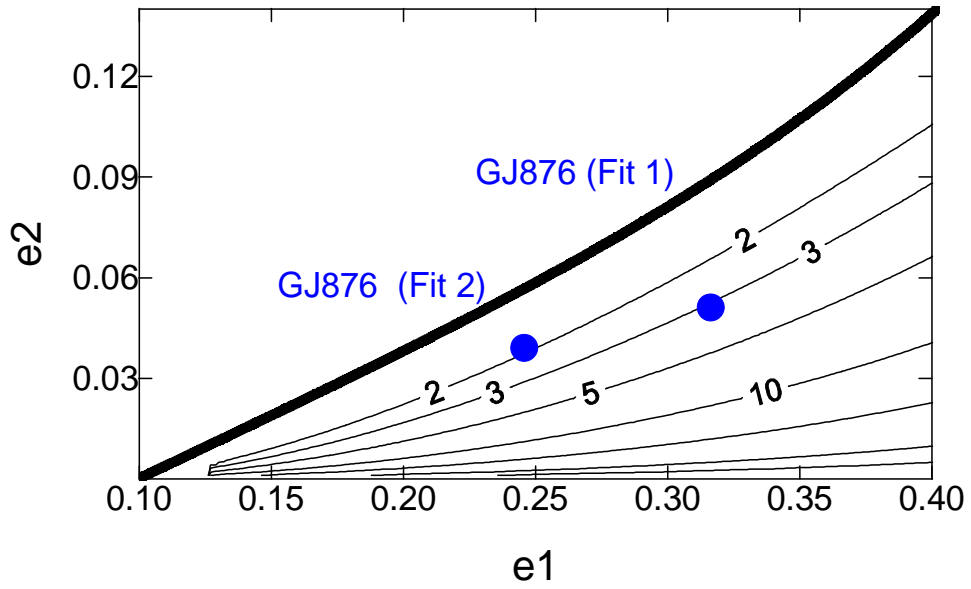


Fig. 3.— Same as previous figure, but for aligned apsidal corotations (i.e.  $\Delta\varpi = 0$ ).

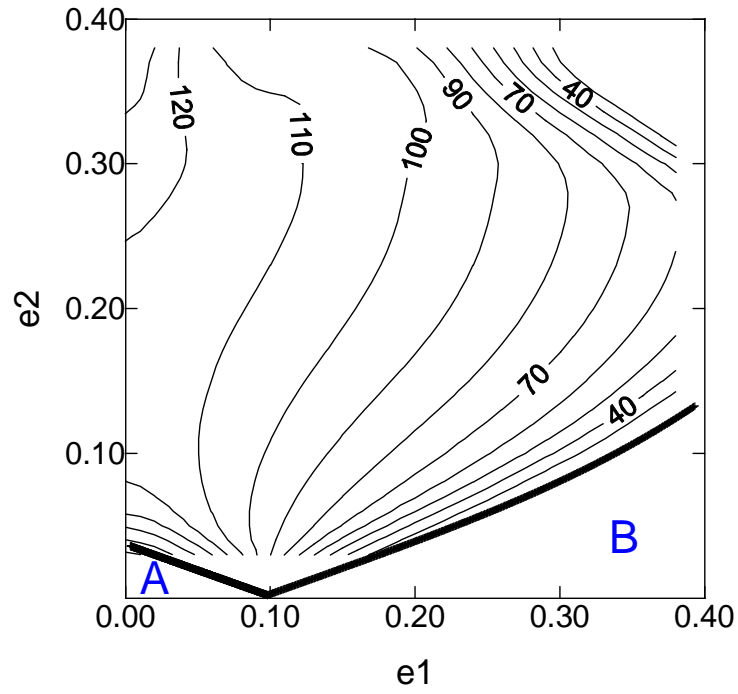
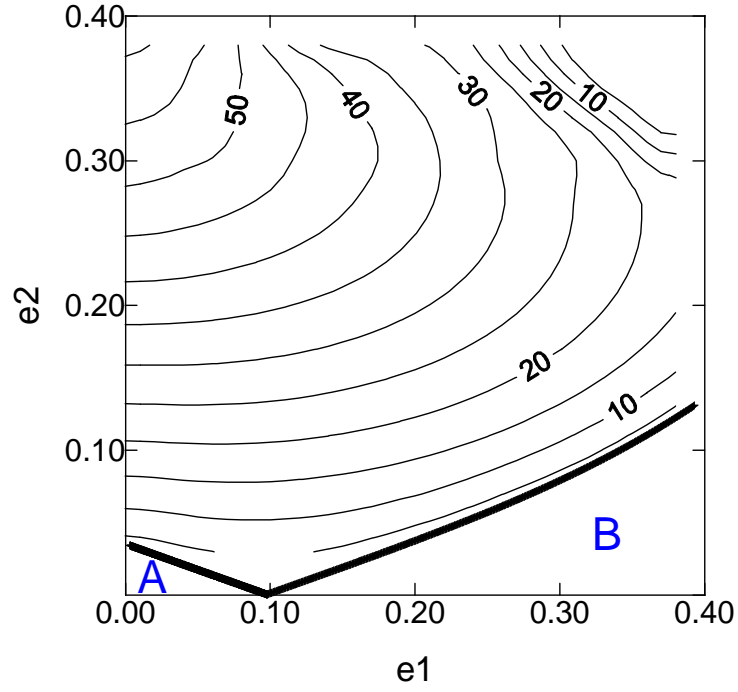


Fig. 4.— Asymmetric apsidal corotation solutions: Values of  $\theta_1$  (top) and  $\varpi_1 - \varpi_2$  (bottom) in the plane  $(e_1, e_2)$ . Angles are given in degrees.

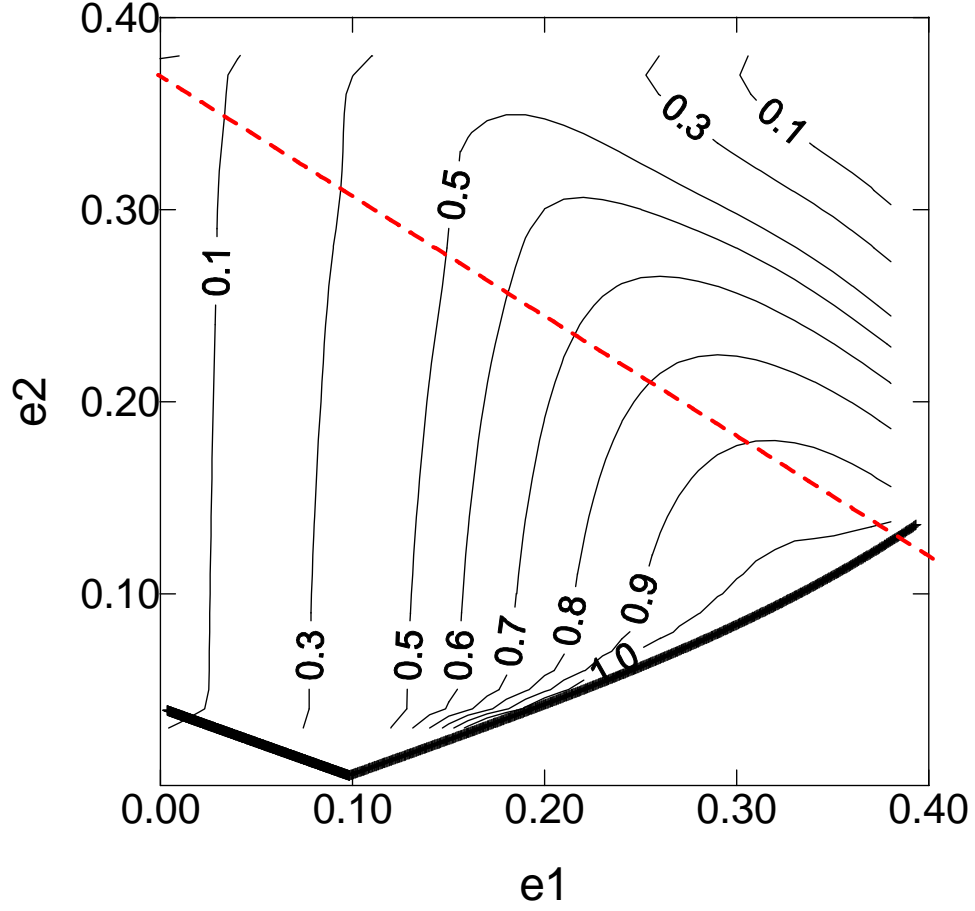


Fig. 5.— Level curves of the mass ratio  $m_2/m_1$  in the asymmetric corotation region. The diagonal broken line marks values of the eccentricities such that  $a_1(1 + e_1) = a_2(1 - e_2)$ .

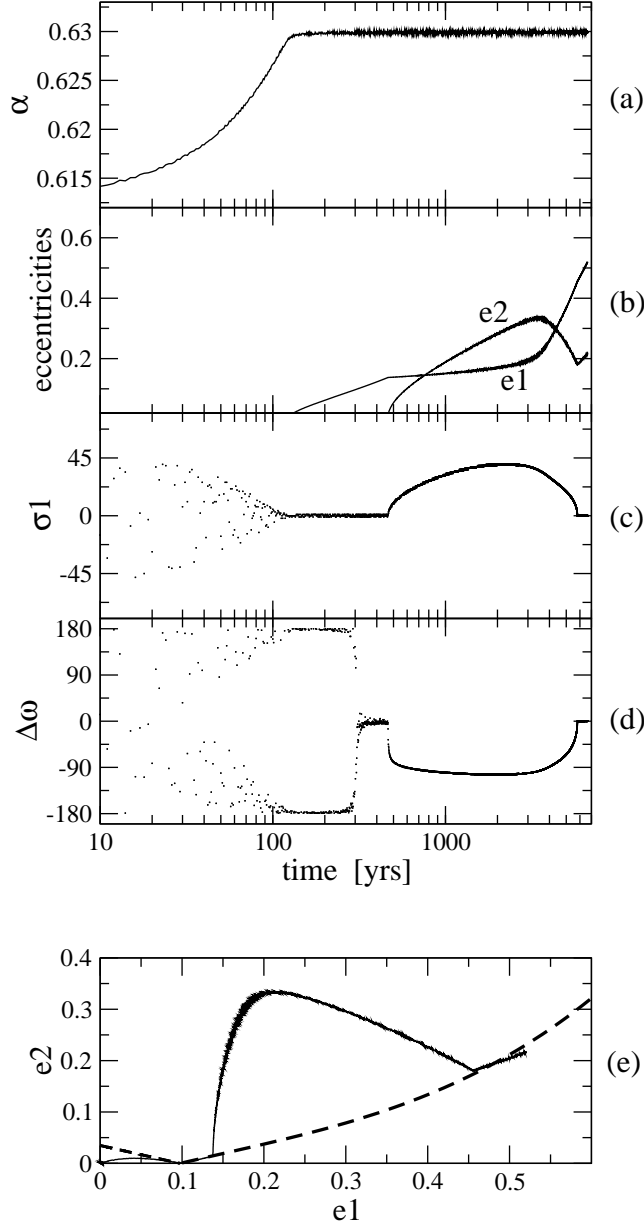


Fig. 6.— Numerical simulation of the capture process in the 2/1 resonance via an orbital migration of the inner planet. Mass ratio of both bodies is equal to  $m_2/m_1 \simeq 0.54$  (similar to the Io-Europa pair). **(a)** Temporal evolution of the ratio of semimajor axes  $\alpha = a_1/a_2$ . **(b)** Eccentricities of both planets as function of time. **(c)** Resonant angle  $\theta_1$ . **(d)** Difference in longitude of pericenter  $\Delta\varpi$ . **(e)** Plane of orbital eccentricities. Broad broken line shows separation between symmetric and asymmetric stationary solutions.

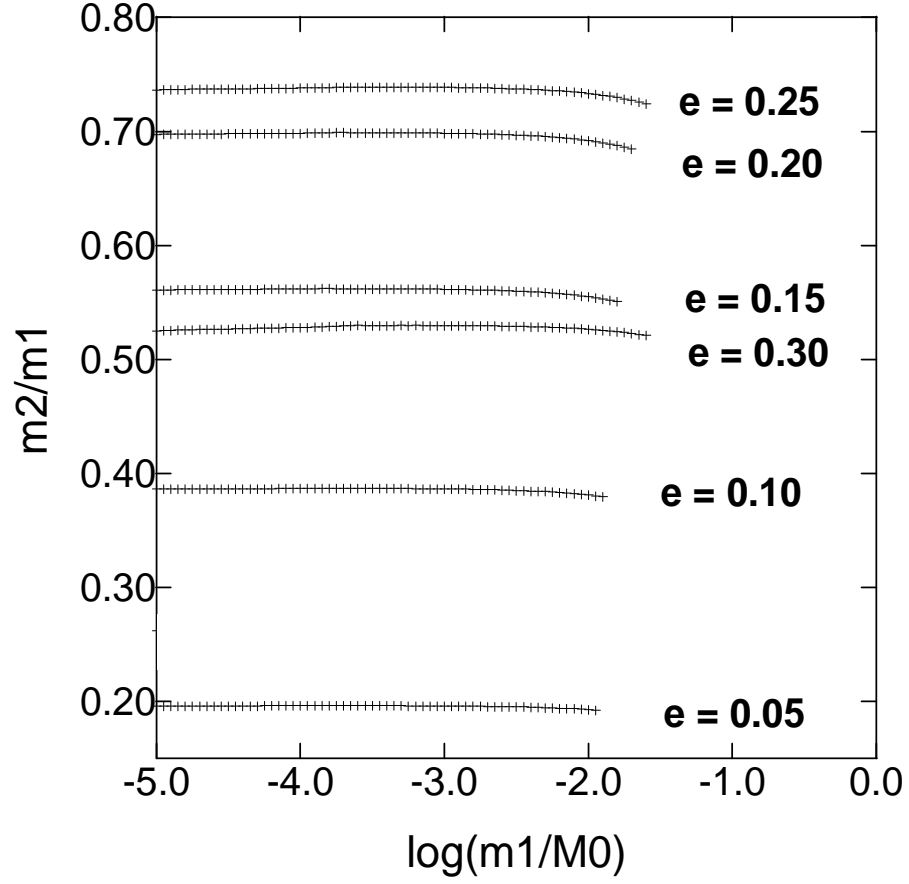


Fig. 7.— Variation of the mass ratio  $m_2/m_1$  as function of  $m_1/M_0$  in stationary solutions with  $e_1 = e_2 = e$ ,

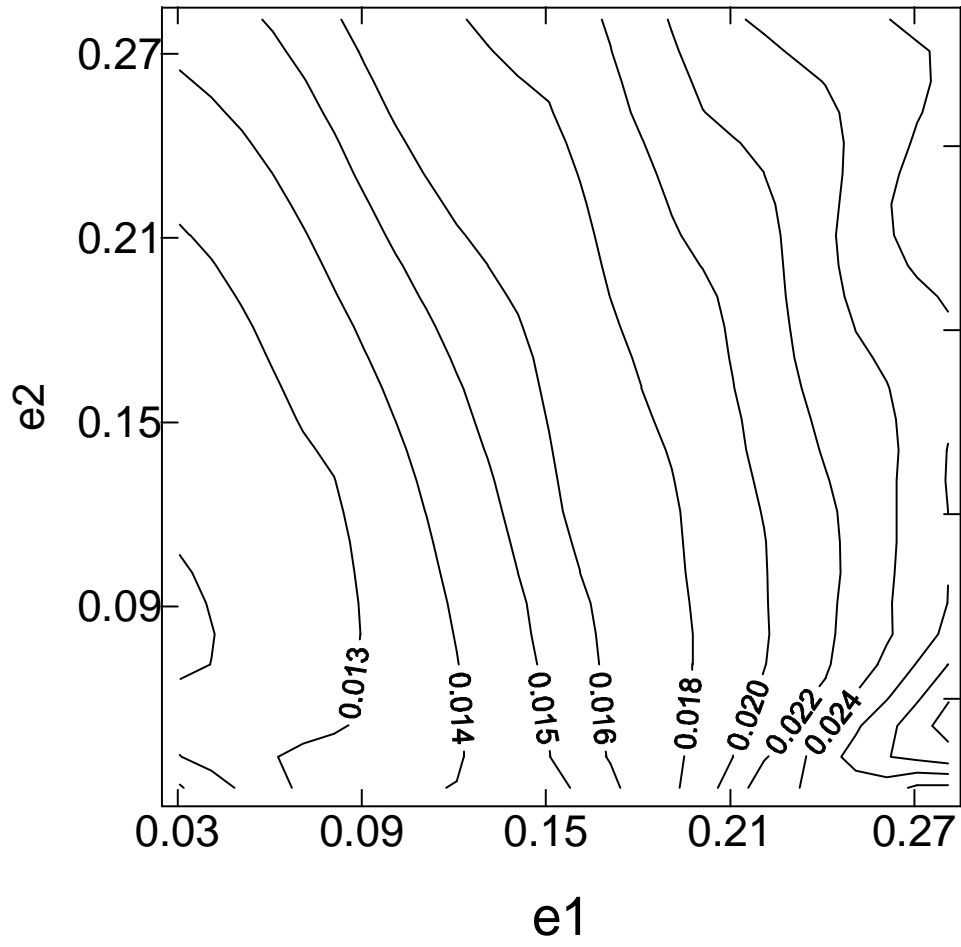


Fig. 8.— In the plane  $(e_1, e_2)$ , maximum value of  $m_1/M_0$  for which stable corotations exist.

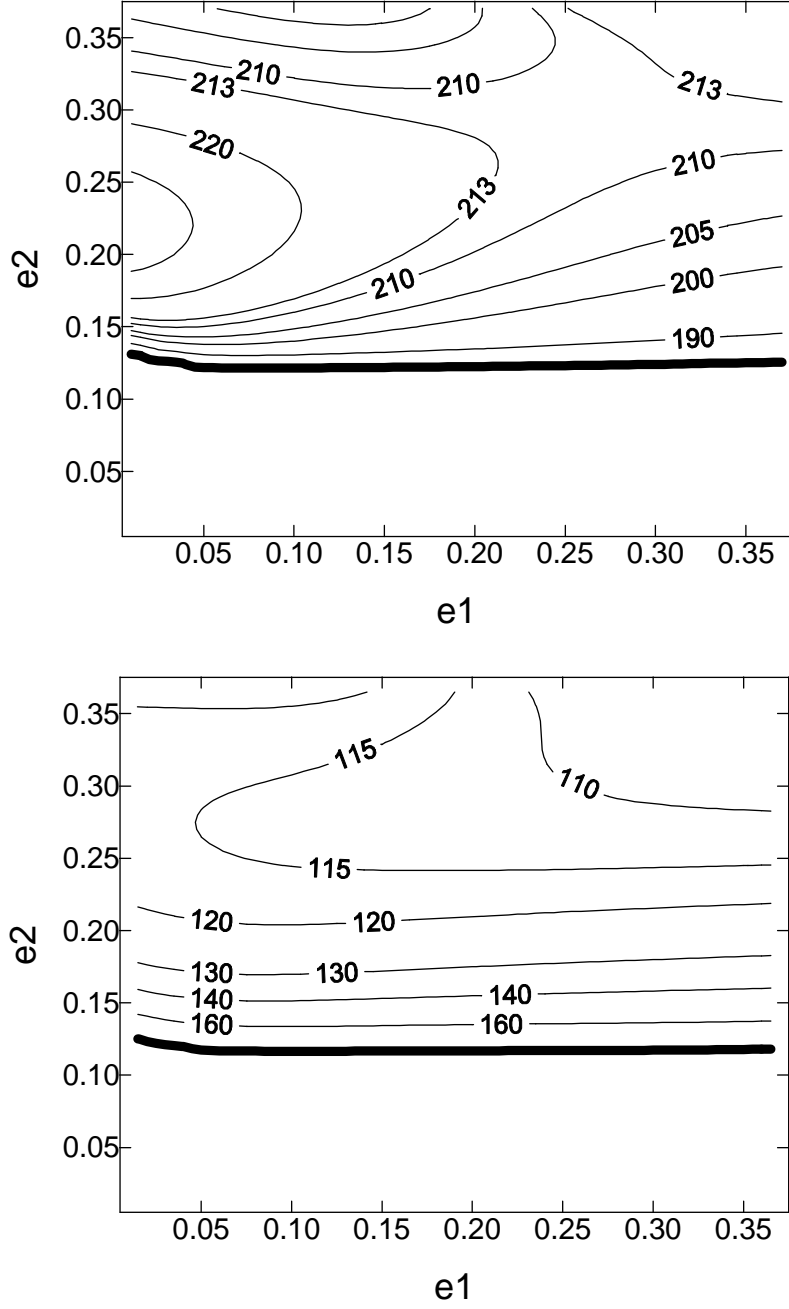


Fig. 9.— Level curves of  $\theta_1$  (top) and  $\Delta\varpi$  (bottom) in the eccentricities-plane for the 3/1 mean-motion resonance. Separation between symmetric and asymmetric regions is given by the broad black curves, below which the stationary solutions correspond to  $\theta_1 = 180$  and  $\Delta\varpi = 180$  degrees.



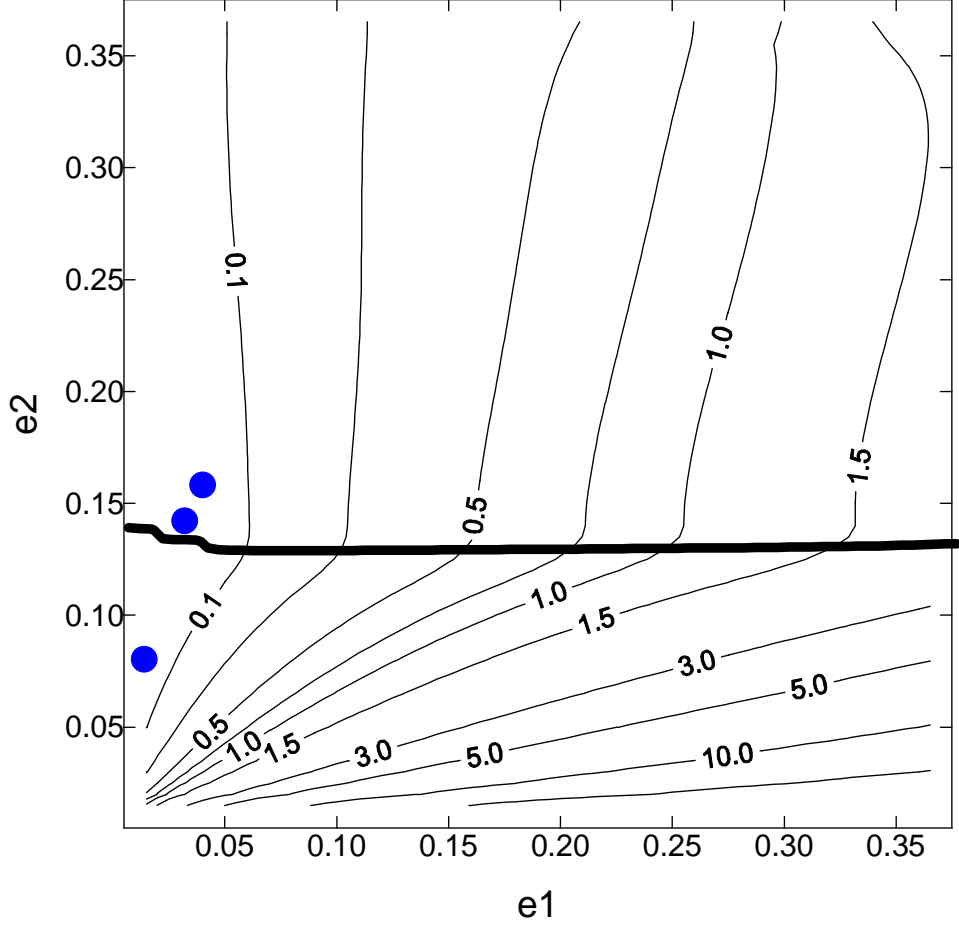


Fig. 10.— Mass-ratio  $m_2/m_1$  of the stationary solutions in the  $(e_1, e_2)$  plane. Note the change in behavior between the apsidal region (below the broad curve) and the asymmetric zone (above). In full circles we also show the three best dynamical fits of the *55Cnc* system.